

Scalar-pseudoscalar meson behavior and restoration of symmetries in SU(3) PNJL model

P. Costa*

*Departamento de Física, Universidade de Coimbra, P-3004-516 Coimbra and
E.S.T.G., Instituto Politécnico de Leiria,
Morro do Lena-Alto do Vieiro, 2411-901 Leiria, Portugal*

M. C. Ruivo and C. A. de Sousa

Departamento de Física, Universidade de Coimbra, P-3004-516 Coimbra, Portugal

H. Hansen

Univ.Lyon/UCBL, CNRS/IN2P3, IPNL “Labo en lutte” , 69622 Villeurbanne Cedex, France

W.M. Alberico

*Dipartimento di Fisica Teorica, University of Torino and INFN,
Sezione di Torino, via P. Giuria 1, I-10125 Torino, Italy*

(Dated: November 2, 2018)

Abstract

The modification of mesonic observables in a hot medium is analyzed as a tool to investigate the restoration of chiral and axial symmetries in the context of the Polyakov-loop extended Nambu–Jona-Lasinio model. The results of the extended model lead to the conclusion that the effects of the Polyakov loop are fundamental for reproducing lattice findings. In particular, the partial restoration of the chiral symmetry is faster in the PNJL model than in the NJL one, and it is responsible for several effects: the meson-quark coupling constants show a remarkable difference in both models, there is a faster tendency to recover the Okubo-Zweig-Iizuka rule, and finally the topological susceptibility nicely reproduces the lattice results around $T/T_c \approx 1.0$.

PACS numbers: 11.10.Wx, 11.30.Rd, 12.38.Aw, 12.38.Mh, 14.65.Bt, 25.75.Nq

Keywords: PNJL model, Restoration of chiral symmetry, Chiral partners

*Electronic address: pcosta@teor.fis.uc.pt

I. INTRODUCTION

In recent years several studies have been developed, which are concerned with the properties of matter under extreme conditions of density and/or temperature: the restoration of symmetries (e.g., the chiral symmetry) and the phenomenon of deconfinement, which might be achieved in ultrarelativistic heavy-ion collisions or in the interior of neutron stars, deserves special attention. Properties of hadrons, in particular, of mesons, propagating in a hot or dense medium can shed light on the occurrence of the expected phenomena [1, 2, 3, 4, 5]. For example, a criterion to identify an effective restoration of chiral (axial) symmetry is to look for the degeneracy of the respective chiral partners [6].

The study of meson properties, in the $SU_f(2)$ sector, around the critical region where the phase transition takes place, was performed in Ref. [7], in the framework of the modified Nambu–Jona-Lasinio model including the Polyakov loop (the so-called PNJL model) [8, 9, 10, 11, 12, 13, 14, 15, 16, 17, 18]. In the PNJL model, quarks are simultaneously coupled to the chiral condensate and to the Polyakov loop, so the model incorporates features of both chiral and \mathbb{Z}_{N_c} symmetry breaking [7]. The coupling to the Polyakov loop is fundamental for reproducing lattice results on QCD thermodynamical quantities [13], since it produces a suppression of the unphysical colored states (one or two quark states), which should not contribute to the thermodynamics below the critical temperature.

In this paper, we intend to extend the investigation of light scalar and pseudoscalar mesons at finite temperature, generalizing previous works to the $SU_f(3)$ sector. In particular, it will be interesting to compare the properties (e.g., the masses) of the scalar mesons (σ , f_0 , a_0 , and K_0^*) with those of the pseudoscalar nonet (η , η' , π^0 , and K), which can be considered as chiral partners of the former. We focus our attention on the role of the Polyakov loop in determining the behavior with the temperature of these mesons.

An interesting open question we wish to address is whether both chiral $SU(N_f)\otimes SU(N_f)$ and axial $U_A(1)$ symmetries are restored and which observables could carry information about these restorations. Moreover, we shall investigate the role of the $U_A(1)$ anomaly which, as is well known, is responsible for the flavor mixing effect that removes the degeneracy among several mesons. The $U_A(1)$ symmetry does not exist at the quantum level being explicitly broken by the axial anomaly [19] which, in turn, can be described at the semiclassical level by instantons [20].

The flavor mixing induced by the presence of the axial anomaly causes a violation of the Okubo-Zweig-Iizuka rule, both for scalar and pseudoscalar mesons, hence the restoration of axial symmetry should have relevant consequences on the phenomenology of the mesonic mixing angles as well as on the topological susceptibility. Also in this context the addition of the Polyakov loop might influence the tendency toward the recovery of the pseudoscalar and scalar mixing angles, already evaluated within the pure NJL model.

The paper is organized as follows: in Sec. II, we present the model Lagrangian of PNJL in $SU_f(3)$ including the 't Hooft interaction term; specific subsections are dedicated to the gap equations, and to the properties (masses and mixing angles) of the pseudoscalar and scalar meson nonets. In Sec. III, we show our results, starting with a discussion on the characteristic temperatures and the role played by the strange components; then we display the mesonic masses, the meson-quark coupling constants, and the topological susceptibility. Our conclusions are reported in Sec. IV.

II. MODEL AND FORMALISM

A. The PNJL model with three flavors

We perform our calculations in the framework of an extended $SU_f(3)$ PNJL Lagrangian, which includes the 't Hooft instanton induced interaction term that breaks the $U_A(1)$ symmetry; moreover quarks are coupled to a (spatially constant) temporal background gauge field representing the Polyakov loop [21, 22, 23]

$$\begin{aligned} \mathcal{L}_{PNJL} = & \bar{q}(i\gamma^\mu D_\mu - \hat{m})q + \frac{1}{2} g_S \sum_{a=0}^8 [(\bar{q} \lambda^a q)^2 + (\bar{q} i \gamma_5 \lambda^a q)^2] \\ & + g_D \{ \det [\bar{q} (1 + \gamma_5) q] + \det [\bar{q} (1 - \gamma_5) q] \} \\ & - \mathcal{U}(\Phi[A], \bar{\Phi}[A]; T). \end{aligned} \quad (1)$$

Here, $q = (u, d, s)$ is the quark field with three flavors ($N_f = 3$) and three colors ($N_c = 3$), $\hat{m} = \text{diag}(m_u, m_d, m_s)$ is the current quark mass matrix, and λ^a are the flavor $SU_f(3)$ Gell-Mann matrices ($a = 0, 1, \dots, 8$), with $\lambda^0 = \sqrt{\frac{2}{3}} \mathbf{I}$. The covariant derivative is defined as $D^\mu = \partial^\mu - iA^\mu$, with $A^\mu = \delta_0^\mu A^0$ (Polyakov gauge); in Euclidean notation $A^0 = -iA_4$. The strong coupling constant G_{Strong} is absorbed in the definition of $A^\mu(x) = G_{Strong} \mathcal{A}_a^\mu(x) \frac{\lambda_a}{2}$, where \mathcal{A}_a^μ is the $(SU_c(3))$ gauge field and λ_a are the (color) Gell-Mann matrices.

The Polyakov loop field Φ appearing in the potential term of (1) is related to the gauge field through the gauge covariant average of the Polyakov line [10, 13]

$$\Phi(\vec{x}) = \langle\langle l(\vec{x}) \rangle\rangle = \frac{1}{N_c} \text{Tr}_c \langle\langle L(\vec{x}) \rangle\rangle, \quad (2)$$

where

$$L(\vec{x}) = \mathcal{P} \exp \left[i \int_0^\beta d\tau A_4(\vec{x}, \tau) \right]. \quad (3)$$

The Polyakov loop is an order parameter for the restoration of the \mathbb{Z}_3 (the center of $\text{SU}_c(3)$) symmetry of QCD and is related to the deconfinement phase transition: \mathbb{Z}_3 is broken in the deconfined phase ($\Phi \rightarrow 1$) and restored in the confined one ($\Phi \rightarrow 0$) [24, 25, 26].

Here, it is important to make some remarks about the applicability of the PNJL model. Beyond the chiral pointlike coupling between quarks, in the PNJL model, the gluon dynamics is reduced to a simple static background field representing the Polyakov loop (see details in Refs. [7, 13]). This scenario cannot be expected to work outside a limited range of temperatures. Indeed, at large temperatures it is expected that transverse gluons start to be thermodynamically active degrees of freedom, but they are not taken into account in the PNJL model. Since, as concluded in Ref. [27], transverse gluons start to contribute significantly for $T > 2.5 T_c$, where T_c is the deconfinement temperature, we can assume that the range of applicability of the model is roughly limited to $T \leq (2 - 3)T_c$.

Concerning the effective potential for the (complex) Φ field, there exist in the literature different choices [13, 15, 23]: we decided to adopt the one proposed in Ref. [15] [see Eq. 4], which is known to give sensible results [15, 16]. In particular, it reproduces, at the mean field level, results obtained in lattice calculations. The potential reads

$$\frac{\mathcal{U}(\Phi, \bar{\Phi}; T)}{T^4} = -\frac{a(T)}{2} \bar{\Phi}\Phi + b(T) \ln[1 - 6\bar{\Phi}\Phi + 4(\bar{\Phi}^3 + \Phi^3) - 3(\bar{\Phi}\Phi)^2] \quad (4)$$

where

$$a(T) = a_0 + a_1 \left(\frac{T_0}{T} \right) + a_2 \left(\frac{T_0}{T} \right)^2 \quad \text{and} \quad b(T) = b_3 \left(\frac{T_0}{T} \right)^3. \quad (5)$$

We notice that in the mean field approximation the Polyakov loop field $\Phi(\vec{x})$ simply coincides with its expectation value $\Phi = \text{const.}$, which minimizes the potential (4). The parameters of the effective potential \mathcal{U} are given in Table I. These parameters have been fixed in order to reproduce the lattice data for the expectation value of the Polyakov loop and QCD thermodynamics in the pure gauge sector [28, 29].

a_0	a_1	a_2	b_3
3.51	-2.47	15.2	-1.75

TABLE I: Parameters for the effective potential in the pure gauge sector (Eq. (4)).

The parameter T_0 is the critical temperature for the deconfinement phase transition within a pure gauge approach: it was fixed to 270 MeV, according to lattice findings. Different criteria for fixing T_0 are available in the literature, like in Ref. [18], where an explicit N_f dependence of T_0 is presented by using renormalization group arguments. Besides, we notice that the Polyakov loop computed on the lattice with (2+1) flavors and with fairly realistic quark masses is very similar to the $SU_f(2)$ case [29]. Hence, we choose to keep for the effective potential $\mathcal{U}(\Phi, \bar{\Phi}; T)$ the same parameters which were used in $SU_f(2)$ PNJL [15], including T_0 .

Since one of the purposes of the present paper is to estimate the effect of the coupling of the Polyakov loop to quarks with NJL 4-point interactions, we choose to compare the NJL and PNJL models on a relative temperature scale T/T_c^x , where T_c^x is a characteristic temperature that can be derived in both models (here, the chiral crossover location). This choice is justified along the lines of the Ginsburg-Landau effective theory, where characteristic temperatures cannot be absolutely compared between two models of the same universality class. Besides, as noticed in Refs. [7, 18] the T_0 dependence of the results is mild. In the present context the physical outcomes are not dramatically modified when one changes T_0 ¹. Hence the choice $T_0 = 270$ MeV appears to be preferable here, since it ensures an almost exact coincidence between chiral crossover and deconfinement at zero chemical potential, as observed in lattice calculations.

With the present choice of the parameters, Φ and $\bar{\Phi}$ are always lower than one in the pure gauge sector. In any case, in the range of applicability of our model ($T \leq 2.5 T_c$), there is a good agreement between our results and the lattice data for Φ .

Let us anticipate that, at $T = 0$, it can be shown that the minimization of the grand potential leads to $\Phi = \bar{\Phi} = 0$. So, the quark sector decouples from the gauge one, and the model is fixed by the coupling constants g_S, g_D , the cutoff parameter Λ , which regularizes

¹ The choice of T_0 certainly deserves investigations beyond the scope of this paper.

the divergent integrals, and the current quark masses m_i . The parameter set used here is $m_u = m_d = 5.5$ MeV, $m_s = 140.7$ MeV, $g_S \Lambda^2 = 3.67$, $g_D \Lambda^5 = 12.36$ and $\Lambda = 602.3$ MeV (for details see Ref. [30]).

B. Gap equations

From the Lagrangian (1) in the mean field approximation it is straightforward (see Ref. [31]) to obtain effective quark masses (the gap equations) given by

$$M_i = m_i - 2g_S \langle \bar{q}_i q_i \rangle - 2g_D \langle \bar{q}_j q_j \rangle \langle \bar{q}_k q_k \rangle, \quad (6)$$

where the quark condensates $\langle \bar{q}_i q_i \rangle$, with $i, j, k = u, d, s$ (to be fixed in cyclic order), have to be determined in a self-consistent way. The last term on the right-hand side derives from the determinantal piece in the Lagrangian, which clearly induces a flavor mixing in the constituent quark masses M_i . So, taking already into account Eq. (6), the PNJL grand canonical potential density in the $SU_f(3)$ sector can be written as

$$\begin{aligned} \Omega = \Omega(\Phi, \bar{\Phi}, M_i; T, \mu) = & \mathcal{U}(\Phi, \bar{\Phi}, T) + g_S \sum_{\{i=u,d,s\}} \langle \bar{q}_i q_i \rangle^2 + 4g_D \langle \bar{q}_u q_u \rangle \langle \bar{q}_d q_d \rangle \langle \bar{q}_s q_s \rangle \\ & - 2N_c \sum_{\{i=u,d,s\}} \int_{\Lambda} \frac{d^3 p}{(2\pi)^3} E_i - 2T \sum_{\{i=u,d,s\}} \int_{\Lambda} \frac{d^3 p}{(2\pi)^3} (z_{\Phi}^+(E_i) + z_{\Phi}^-(E_i)), \end{aligned} \quad (7)$$

where we have defined $E_i^{(\pm)} = E_i \mp \mu$, the upper sign applying for fermions and the lower sign for antifermions; E_i is the quasiparticle energy for the quark i : $E_i = \sqrt{\mathbf{p}^2 + M_i^2}$; finally, z_{Φ}^+ and z_{Φ}^- are the partition function densities (with the usual notation $\beta = 1/T$)

$$z_{\Phi}^+(E_i) \equiv \text{Tr}_c \ln \left[1 + L^\dagger e^{-\beta E_i^{(+)}} \right] \ln \left\{ 1 + 3 \left(\bar{\Phi} + \Phi e^{-\beta E_i^{(+)}} \right) e^{-\beta E_i^{(+)}} + e^{-3\beta E_i^{(+)}} \right\} \quad (8)$$

$$z_{\Phi}^-(E_i) \equiv \text{Tr}_c \ln \left[1 + L e^{-\beta E_i^{(-)}} \right] \ln \left\{ 1 + 3 \left(\Phi + \bar{\Phi} e^{-\beta E_i^{(-)}} \right) e^{-\beta E_i^{(-)}} + e^{-3\beta E_i^{(-)}} \right\}. \quad (9)$$

It was shown in Ref. [7] that all calculations in the NJL model can be generalized to the PNJL one by introducing the modified Fermi-Dirac distribution functions for particles and antiparticles:

$$f_{\Phi}^{(+)}(E_i) = \frac{\bar{\Phi} e^{-\beta E_i^{(+)}} + 2\Phi e^{-2\beta E_i^{(+)}} + e^{-3\beta E_i^{(+)}}}{\exp\{z_{\Phi}^+(E_i)\}} \quad (10)$$

$$f_{\Phi}^{(-)}(E_i) = \frac{\Phi e^{-\beta E_i^{(-)}} + 2\bar{\Phi} e^{-2\beta E_i^{(-)}} + e^{-3\beta E_i^{(-)}}}{\exp\{z_{\Phi}^-(E_i)\}}. \quad (11)$$

To obtain the mean field equations we must search for the minima of the thermodynamical potential density (7) with respect to $\langle \bar{q}_i q_i \rangle$ ($i = u, d, s$), Φ , and $\bar{\Phi}$. In fact, by minimizing Ω with respect to $\langle \bar{q}_i q_i \rangle$, we obtain the equations for the quark condensates

$$\langle \bar{q}_i q_i \rangle = -2N_c \int_{\Lambda} \frac{d^3 p}{(2\pi)^3} \frac{M_i}{E_i} [1 - f_{\Phi}^{(+)}(E_i) - f_{\Phi}^{(-)}(E_i)]. \quad (12)$$

Furthermore, minimization of Ω with respect to Φ and $\bar{\Phi}$ provides, respectively, the two additional mean field equations [7]

$$0 = T^4 \left\{ -\frac{a(T)}{2} \bar{\Phi} - 6 \frac{b(T) [\bar{\Phi} - 2\Phi^2 + \bar{\Phi}^2 \Phi]}{1 - 6\bar{\Phi}\Phi + 4(\bar{\Phi}^3 + \Phi^3) - 3(\bar{\Phi}\Phi)^2} \right\} - 6T \sum_{\{i=u,d,s\}} \int_{\Lambda} \frac{d^3 p}{(2\pi)^3} \left(\frac{e^{-2\beta E_i^{(+)}}}{\exp\{z_{\Phi}^{+}(E_i)\}} + \frac{e^{-\beta E_i^{(-)}}}{\exp\{z_{\Phi}^{-}(E_i)\}} \right) \quad (13)$$

$$0 = T^4 \left\{ -\frac{a(T)}{2} \Phi - 6 \frac{b(T) [\Phi - 2\bar{\Phi}^2 + \bar{\Phi}\Phi^2]}{1 - 6\bar{\Phi}\Phi + 4(\bar{\Phi}^3 + \Phi^3) - 3(\bar{\Phi}\Phi)^2} \right\} - 6T \sum_{\{i=u,d,s\}} \int_{\Lambda} \frac{d^3 p}{(2\pi)^3} \left(\frac{e^{-\beta E_i^{(+)}}}{\exp\{z_{\Phi}^{+}(E_i)\}} + \frac{e^{-2\beta E_i^{(-)}}}{\exp\{z_{\Phi}^{-}(E_i)\}} \right) \quad (14)$$

This general formalism, presented here for completeness in the grand canonical approach, is going to be employed in the present work with $\mu = 0$. Under this condition, the constraint $\bar{\Phi} = \Phi$ holds.

C. Pseudoscalar and scalar meson nonets

To calculate the meson mass spectrum, we use the same procedure described in detail in Ref. [6]. The model Lagrangian (1) can be put in a form suitable for the usual bosonization procedure, after reducing the six-quark interaction term in order to obtain an effective four-quark interaction. This can be achieved, e.g., by shifting the operator $(\bar{q}\lambda^a q) \longrightarrow (\bar{q}\lambda^a q) + \langle \bar{q}\lambda^a q \rangle$, where $\langle \dots \rangle$ is the vacuum expectation value [31] and by Wick contracting one of the bilinears $(\bar{q}\lambda^a q)$ in the resulting six-quarks interaction term. The following effective quark Lagrangian is thus obtained:

$$\mathcal{L}_{eff} = \bar{q} (i \gamma^{\mu} \partial_{\mu} - \hat{m}) q + \frac{1}{2} S_{ab} [(\bar{q} \lambda^a q)(\bar{q} \lambda^b q)] + \frac{1}{2} P_{ab} [(\bar{q} i \gamma_5 \lambda^a q)(\bar{q} i \gamma_5 \lambda^b q)], \quad (15)$$

where the projectors S_{ab}, P_{ab} are of the form

$$S_{ab} = g_S \delta_{ab} + g_D D_{abc} \langle \bar{q} \lambda^c q \rangle, \quad (16)$$

$$P_{ab} = g_S \delta_{ab} - g_D D_{abc} \langle \bar{q} \lambda^c q \rangle. \quad (17)$$

The constants D_{abc} coincide with the $SU_f(3)$ structure constants for $a, b, c = (1, 2, \dots, 8)$, while $D_{0ab} = -\frac{1}{\sqrt{6}}\delta_{ab}$ and $D_{000} = \sqrt{\frac{2}{3}}$. The bosonization procedure is then realized by integrating out the quark fields in the functional generator associated with the Lagrangian (15) complemented by the coupling to scalar and pseudoscalar bosonic fields. With this procedure the natural degrees of freedom of low-energy QCD in the mesonic sector emerge in the resulting effective bosonic action. By expanding the latter up to second order in the meson fields, one obtains the meson propagators, from which the masses, meson-quark coupling constants and meson decay constants f_M can be evaluated according to the usual definitions (see, for example, Eqs. (21) and (22) of Ref. [32]).

For example, we obtain the inverse propagator for the pion as

$$D_\pi^{-1}(P) = 1 - P_\pi \Pi_{uu}^P(P), \quad (18)$$

where

$$P_\pi = g_S + g_D \langle \bar{q}_s q_s \rangle, \quad (19)$$

and $\Pi_{ab}^P(P)$ is the polarization operator, which in momentum space has the form

$$\Pi_{ab}^P(P) = iN_c \int \frac{d^4 p}{(2\pi)^4} \text{tr}_D [S_i(p)(\lambda^a)_{ij}(i\gamma_5) S_j(p+P)(\lambda^b)_{ji}(i\gamma_5)], \quad (20)$$

with tr_D being now the trace over Dirac matrices. For details concerning the calculations for the other meson propagators, see Ref. [6]. At variance with Ref. [6], here the introduction of the Polyakov loop implies, obviously, the use of the modified Fermi functions f_Φ in the calculation.

The inclusion of the 't Hooft interaction in the PNJL/NJL model allows for flavor mixing; however, by imposing $SU_f(2)$ flavor symmetry (namely, $m_u = m_d$) the off-diagonal coupling strengths that mix the π^0 with η and η' vanish; hence, charged and neutral pions become degenerate in mass, as well as the neutral and charged kaons.

It should be noticed that flavor mixing somewhat entangles the calculation of the η and η' masses and couplings, since it gives rise to a P^2 -dependent mixing angle $\theta_P(P^2)$ [6, 30],

which in our scheme is defined as follows:

$$\begin{pmatrix} \eta \\ \eta' \end{pmatrix} = O(\theta_P) \begin{pmatrix} \eta_8 \\ \eta_0 \end{pmatrix} = \begin{pmatrix} \cos\theta_P & -\sin\theta_P \\ \sin\theta_P & \cos\theta_P \end{pmatrix} \begin{pmatrix} \eta_8 \\ \eta_0 \end{pmatrix}. \quad (21)$$

In the above, η and η' stand for the corresponding physical fields, while η_8 and η_0 are the mathematical objects transforming as octet and singlet states of the $SU_f(3)$ pseudoscalar meson nonet, respectively. By using a standard procedure we get the equation for the mixing angles and for the inverse meson propagators [6].

As shown elsewhere, in the framework of the NJL model [6, 30], the mixing angle θ_P , between the components η_0 and η_8 is P^2 -dependent; hence, one gets different mixing angles at $P^2 = M_\eta^2$ or $P^2 = M_{\eta'}^2$. In the present paper we only discuss the mixing angle at $P^2 = M_\eta^2$; nevertheless, we checked that the behavior of the mixing angle at $P^2 = M_{\eta'}^2$ gives qualitatively similar information.

The same technique used for the pseudoscalar sector can now be directly applied to the scalar resonances. We deal here with nine scalar resonances: three a_0 's, which are the scalar partners of the pions, four κ 's, being the scalar partners of the kaons, and the σ and f_0 , which are similarly associated with the η and η' . As in the pseudoscalar case, we impose the $SU_f(2)$ flavor symmetry, so we have no mixing between the σ and f_0 and the neutral a_0^0 .

As is well known, when the mass of the meson exceeds the sum of the masses of its constituent quarks, the meson can decay in its quark–antiquark pair, hence becoming a resonant state. So, in order to calculate the mass of the resonance, the imaginary part of the propagator must be taken into account as well and, following the standard approximation described in Ref. [33], one can obtain the mass and the corresponding decay width.

III. NUMERICAL RESULTS

A. NJL vs PNJL: Characteristic temperatures

We start our analysis by identifying the characteristic temperatures that separate the different thermodynamic phases in PNJL and NJL models [7]. In the framework of the PNJL model the critical temperature related to the “deconfinement”² phase transition is T_c^Φ and

² The terminology “deconfinement” in our model is used to designate the transition between $\Phi \simeq 0$ and $\Phi \simeq 1$ (see Ref. [7] for a discussion of this point).

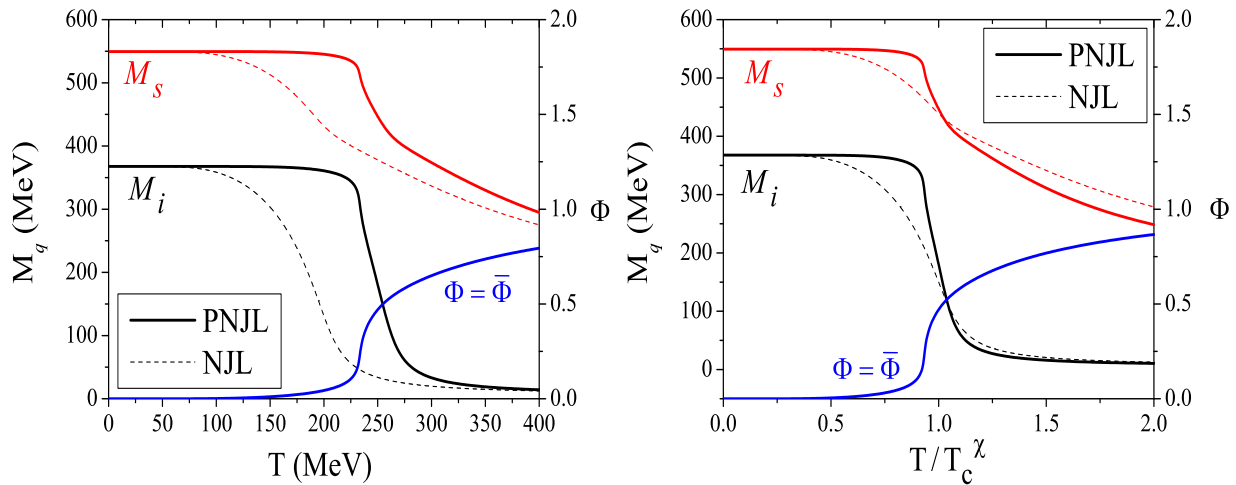


FIG. 1: Left panel: comparison of the quark masses in the PNJL (solid lines) and NJL (dashed lines) models as functions of the temperature; the Polyakov loop crossover is also shown. Right panel: the same as before as a function of the reduced temperature T/T_c^χ .

corresponds to the Φ crossover location (Fig.1). The chiral phase transition characteristic temperatures, T_c^χ , are given in both models by the inflexion points (chiral crossover) of the chiral condensates $\langle \bar{q}_i q_i \rangle$. Since in both situations chiral symmetry is explicitly broken by the presence of nonzero current quark mass terms, chiral symmetry is realized through parity doubling rather than by massless quarks. The effective chiral symmetry restoration [in the $SU_f(2)$ sector] is signaled by the degeneracy of the chiral partners (π , σ) and (η , a_0) or, strictly speaking, by the merging of their spectral functions [6, 7].

In order to compare the NJL and PNJL results, it is useful to follow the evolution of the observables as functions of the temperature, expressed both in physical units (MeV) as well as rescaled in units of a characteristic temperature. For the latter we choose the corresponding T_c^χ in NJL and PNJL, and most figures will be shown versus T/T_c^χ , which allows a better understanding of the relevant differences between NJL and PNJL models. Indeed, we are not interested in discussing absolute quantities but rather in comparing the behavior, below and above T_c^χ , of the mesonic properties; the key point under investigation is the effective restoration of symmetries, as well as the influence of the Polyakov loop on the phase transition.

In Table II we quote the characteristic temperatures: the effective chiral symmetry

Model	T_c^χ [MeV]	T_c^Φ [MeV]	T_{Mott}^π [MeV]	T_{Mott}^σ [MeV]
PNJL	250	233	267	237
NJL	196	—	212	160

TABLE II: Characteristic temperatures in the NJL and PNJL models at $T_0 = 270$ MeV and zero chemical potential.

restoration temperature, the deconfinement temperature, and the Mott temperatures for the pion and the sigma both in PNJL and NJL models. We remind the reader that the Mott transition is associated with the composite nature of the mesons: at the Mott temperature the decay of a meson into a $\bar{q}q$ pair becomes energetically favorable.

As already noticed in the $SU_f(2)$ PNJL model [13], T_c^Φ differs by only a few MeV's from T_c^χ . In $SU_f(3)$ this difference is 17 MeV. From Table II, we also see that the characteristic temperatures obtained in PNJL are much larger than the lattice result for the chiral/deconfinement phase transition in (2+1) flavors QCD ($T_c \simeq 170$ MeV). It was pointed out in Ref. [7] that the difference between T_c^Φ and T_c^χ is due to the choice of the regularization procedure; we apply here the three-dimensional momentum cutoff to both the zero and the finite temperature contributions. Notice also that a different type of regularization can lower T_c^χ [34]. Another important aspect contributing to the present high value of T_c^χ is the fact that we do not rescale the parameter T_0 to a smaller value after introducing quarks in the system. Indeed, we checked that using the lower value $T_0 = 187$ MeV suggested in Ref. [18], smaller characteristic temperatures, T_c^Φ and T_c^χ are obtained. However, we prefer to adopt the higher T_0 value since it gives a smaller difference between the critical points of the two transitions. Nevertheless, once we are interested in the general properties of mesons, the absolute value of the critical temperature is not so relevant: indeed, these properties are independent of the specific value of T_c^χ and a different value of T_0 does not change the conclusions.

B. The strangeness in PNJL

In Fig. 1 we plot the masses of the strange and nonstrange quarks and the Polyakov loop as functions of the temperature. At temperatures around T_c^χ , in both models, the mass of

the light quarks drops to the current quark mass, indicating a smooth crossover from the chirally broken to an approximate chirally symmetric phase: we have a partial restoration of chiral symmetry. This dropping is more pronounced in the PNJL model than in the NJL one, indicating that the transition toward the partial chirally restored phase is faster in the former. The strange quark mass shows a behavior very similar to the one of the nonstrange quarks, with a significant decrease above T_c^x ; however, its mass is still far away from the strange current quark mass. One can say that chiral symmetry shows a slow tendency to get restored in the strange sector even if this tendency is faster in the PNJL model. As in the NJL model, for what concerns the strange sector [6] and since $m_u = m_d < m_s$, the (sub)group $SU(2) \otimes SU(2)$ is a much better symmetry of the Lagrangian (1).

Nevertheless, the fact that the masses of the quarks drop faster around T_c^x in the PNJL model is important for the mesonic properties (for example it could modify the survival of mesonic bound states in the plasma phase). Moreover, due to the strange components of some mesons, the behavior of the strange quark mass (modified by the Polyakov loop) is important for their properties, as well as for other observables related to the axial anomaly (as noticed in [34] the topological susceptibility is strongly influenced by the strange sector).

C. Mesonic masses and mixing angles

In Fig. 2 we plot the masses of the pseudoscalar mesons and of the respective scalar chiral partners as functions of the reduced temperature T/T_c^x . The first evidence emerging from these figures is that the behavior of the mesonic masses in PNJL looks, qualitatively, very similar to the corresponding one in NJL [30, 35]. Hence, the results in the two models will deserve, in general, similar conclusions, although there are some quantitative differences with a non-trivial meaning that will be commented on below.

In the upper panel of Fig. 2 we plot the masses of the scalar and pseudoscalar mesons (σ, a_0, π, η) (upper panel), f_0, η' (middle panel) and finally the masses for the K meson and its chiral partner κ (lower panel), both in the NJL and PNJL models. The lower limits of the continua pertaining to each meson are also shown. In fact, the continuum starts at the crossing of the π, σ , and η lines with the quark threshold $2M_u$ (upper panel), of η' with $2M_s$ (middle panel) and of the K line with $M_u + M_s$.

We will now analyze the general behavior of the mesons and mixing angles, starting by

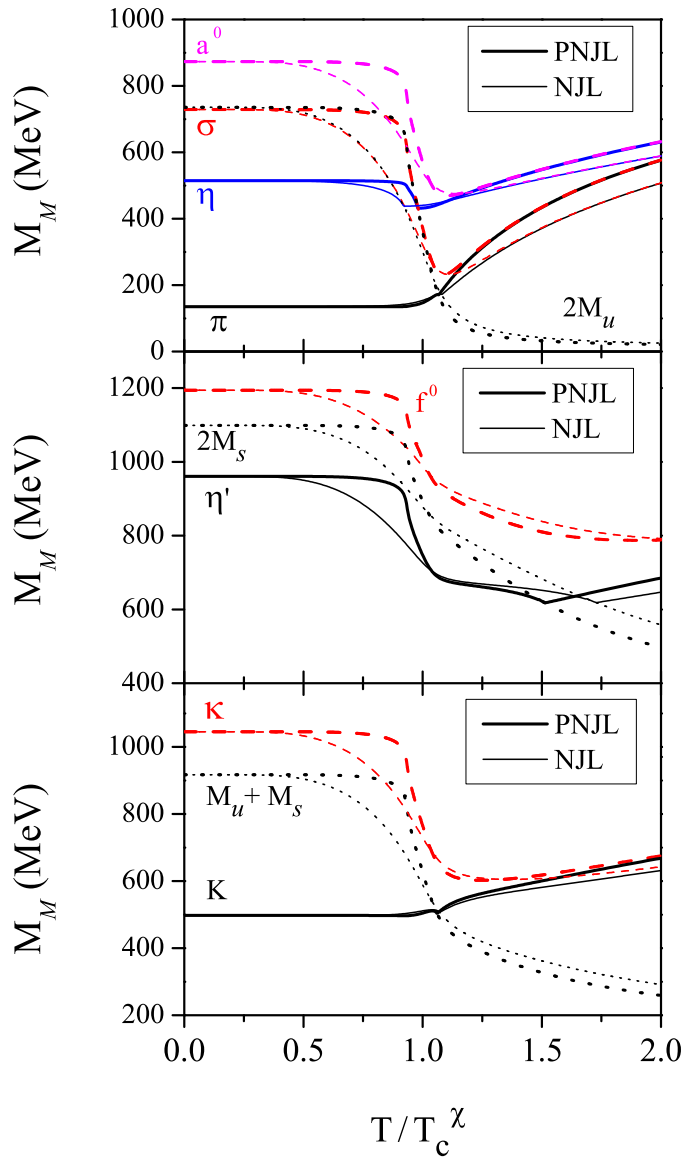


FIG. 2: Comparison of the pseudoscalar and scalar mesons masses in the PNJL (thick lines) and NJL (thin lines) models as functions of the reduced temperature T/T_c^χ . In the upper panel the a_0 (dashed line), σ (dotted-dashed line), η and π (continuous lines) are shown, together with the $2M_u$ mass (dotted lines). In the middle panel f_0 (dashed line) and η' (continuous line) are shown and compared with the $2M_s$ mass (dotted line). In the lower panel the κ (dashed line) and K (continuous line) masses are compared with $M_u + M_s$ (dotted line).

emphasizing what both models have in common. Concerning the pseudoscalar mesons, it is found that they are bound states at low temperature (with the exception of the η' meson, which is always above the continuum $\omega_u = 2M_u$), but at the respective Mott temperatures

they become unbound (see Table II); as usual, for the π and K mesons this occurs at approximately the same temperature in both models ($T_{Mott}^{K-PNJL(NJL)} = 266$ (210) MeV). The σ is the only scalar meson that can be considered as a true (slightly) bound state for small temperatures (the other mesons being always resonant states) and turns into a resonance at the corresponding Mott temperature (see Table II).

Concerning the pseudoscalar mixing angle θ_P , it is found that, as the temperature increases, it approaches the ideal value $\theta_P = -54.736^\circ$, although never reaching it (see Fig. 3). As a consequence, the quark content of the mesons η and η' changes remarkably, although a small percentage of mixing always remains: the η eventually becomes almost nonstrange, while the opposite happens to η' [6, 35]. The scalar mixing angle θ_S exhibits a similar tendency, the ideal mixing angle $\theta_S = 35.264^\circ$ never being reached in the range of temperatures studied here (see Fig. 3); hence, the strange component of the σ meson decreases but never vanishes, and f_0 becomes almost purely strange.

Our main concern in this paper are the modifications introduced by the Polyakov loop on the results obtained in the pure NJL model, which are not new (see for instance [6, 30, 34, 35]); yet, some comments are in order concerning the behavior of the mixing angles, keeping also in mind some recent contributions to this subject in the framework of other models [43, 44]. The mixing angles are very sensitive to the medium effects, in particular to the influence of the medium on the strange quark mass: this might also explain why some aspects of the in-medium behavior of θ_S and θ_P are not the same in different models or situations.

First of all it should be noted that the mixing angles depend on the masses of the mesons and, for the sake of illustration, the angles plotted here are θ_S , depending on the mass of the σ meson and θ_P , depending on the mass of the η meson. Since the σ meson has a small strangeness component, its behavior is essentially driven by the decrease of the nonstrange quark mass; on the contrary, the η has a stronger strangeness component, and its behavior is affected not only by the fast decrease of the nonstrange quark mass, but also by the slow decrease of the strange quark mass. Consequently, the mass of the σ decreases more rapidly than the one of the η and, as a result, θ_S gets closer than θ_P to the respective ideal value, as can be seen in Fig. 3. Notice that there is even a slight increase of θ_P at about $T \simeq 1.75 T_c^x$, the temperature at which the η meson enters into the strange quark continuum ($m_\eta \geq 2M_s$).

The evolution of the strangeness content of η , η' determines which one will become non-

strange, hence behaving as the chiral axial partner of the π . For example, the finite temperature behavior of θ_P leads to the identification of the η as the chiral axial partner of the π in Refs. [40, 41] and [6, 30, 34, 35], but the opposite is found in Refs. [42, 43]. An interesting situation was reported in Refs. [6, 30, 35], for neutron matter in β equilibrium, where the strange quark mass decreases more rapidly than in symmetric nuclear matter. As a consequence, the pseudoscalar mixing angle changes sign and approaches the positive ideal value, while η and η' exchange identities, the η' becoming nonstrange and exhibiting a tendency to degenerate with the pion. A level crossing of the pseudoscalar mixing angle and exchange of identities of η, η' was also found in Ref. [41], and a similar effect for the scalar angle is reported in Ref. [43].

Recently, a study of the mixing angles in the framework of a Schwinger-Dyson approach [44], using a separable interaction, established a connection between the behavior of θ_P and the fastness of restoration of the axial symmetry, characterized by the drop of the topological susceptibility. Since in the NJL model the topological susceptibility is proportional to the strange quark condensate, this result is compatible with our remark, which relates the behavior of the mixing angles to the strange quark mass evolution. We observe that in the PNJL model there is a faster restoration of chiral symmetry, both in the nonstrange and strange sectors, leading to a modification of the in-medium behavior of the mixing angles, meson masses, coupling constants, and topological susceptibility, as we will discuss below. However, the modification induced by the Polyakov loop is limited to a range of temperatures around the critical one ($\sim 0.75 T_c^x - 1.5 T_c^x$), and it is not strong enough to alter the sign of the mixing angles. Having in mind the lack of experimental information on the behavior of the observables discussed here, a comparative study of θ_S and θ_P in different models and situations is desirable.

Let us now analyze the evolution of the mesonic properties in connection with the possible restoration of symmetries. In the present work, the mesonic behavior is driven only by the degree of restoration of chiral symmetry in the different sectors. This does not exclude that other effects, not taken into account here, might influence its behavior. It can be seen in Fig. 2 (upper panel) that the partners (π, σ) and (η, a_0) become degenerate at almost the same temperature. In both models, this behavior is the signal of the effective restoration of chiral symmetry in the nonstrange sector.

On the contrary, the η' and f_0 masses do not show a tendency to converge in the region

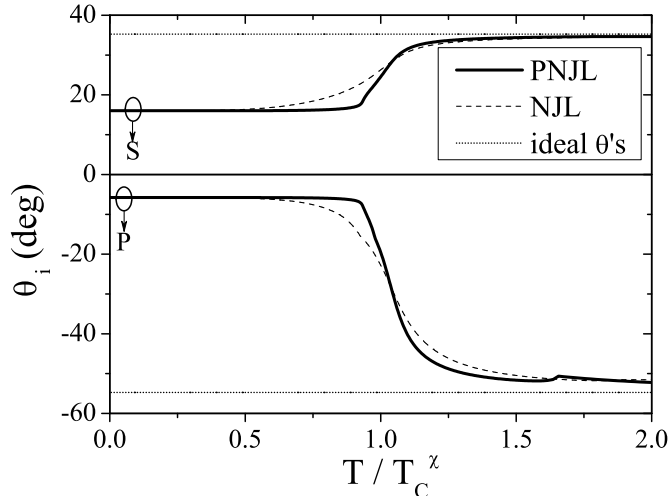


FIG. 3: Scalar and pseudoscalar mixing angles as a function of the reduced temperature T/T_c^x for the PNJL (solid lines) and NJL (dashed lines) models; the ideal mixing angles are also shown (dotted lines).

of temperatures studied, a behavior that reflects the reluctance of chiral symmetry to get restored in the strange sector. In fact, due to the behavior of the mixing angles, f_0 and η' become essentially strange as the temperature increases. Moreover, as it has been shown in Ref. [34], even when the dynamically broken chiral symmetry is restored in all sectors (and differently from what is found for nonstrange chiral partners) a sizable difference between the masses of these mesons survives, a fact due to the high value of the current strange quark mass used here ($m_s = 140.7$ MeV). Indeed, at high temperatures $m_{f_0}^2 \simeq m_{\eta'}^2 + 4m_s^2$, thus explaining the observed behavior. Finally, we focus on the κ meson (Fig. 2 lower panel): it is always an unbound, resonant state and, as the temperature increases, it tends to become degenerate in mass with the K meson, but at a temperature of the order of $1.5 T_c^x$ (in PNJL, and higher in NJL). In summary, the masses of the mesons that become less strange, σ and η , converge, respectively, with those of the non strange, π^0 and a_0 . The convergence of the chiral partners κ and K , which have a $\bar{u}s$ structure, occurs at higher temperatures, and is probably slowed down by the small decrease of the strange quark mass, M_s .

Concerning the axial symmetry, its effective restoration should be signaled by the vanishing of the observables related to the anomaly, like the mixing angles, the gap between the masses of the chiral partners of the $U_A(1)$ symmetry, and the topological susceptibility. For

the observables so far analyzed, we notice that although in both models the anomaly effects exhibit a tendency to decrease, a full restoration of the axial symmetry is not achieved: the masses of the partners (π, η) and (σ, a_0) , although getting close at high temperatures, do not converge and the mixing angles never reach the ideal values. This was indeed expected since, in the framework of the NJL model, it has been shown that only with additional assumptions (for example, by choosing a temperature dependent anomaly coefficient [6] or by using a regularization where the cutoff goes to infinity at $T \neq 0$ [34]) the restoration of the axial symmetry can be achieved.

Let us now comment on the differences between the results of the two models. The new feature of the PNJL model is that the faster decrease of the quark condensates leads to a faster partial restoration of chiral symmetry. Also the analysis of the mesonic masses shows that a faster effective restoration of this symmetry, in the nonstrange sector, is achieved, as can be seen in Fig. 2. In fact, in the NJL model the effective chiral symmetry restoration for the nonstrange sector occurs at $T_{eff} = 1.3 T_c^\chi$ while, in the PNJL model, $T_{eff} = 1.2 T_c^\chi$ (again we do a relative comparison between the two models: T_{eff} and T_c^χ are derived and compared for each model, respectively); for the $K - \kappa$ sector, the temperatures are about 1.5 (NJL) and 2 (NJL) times the corresponding characteristic temperature. Finally, although the axial chiral partners do not converge, in the PNJL model, the masses of (π, η) become closer than in NJL, as well as those of (σ, a_0) . From Fig. 3 we can also see that around T_c^χ the mixing angles θ_P and θ_S approaches faster the ideal angle in the PNJL model than in the NJL one. This is an indication that, although axial symmetry is not restored in the range of temperatures studied, the tendency to restore this symmetry is slower in the NJL model.

D. Coupling constants

In Fig.4 we plot the values of the π , K , η and σ coupling constants. We observe a striking behavior at the Mott temperature for each meson: the coupling strengths approach zero for $T \rightarrow T_{Mott}^{Meson}$ [32]. This is due to the fact that the polarization displays a kink singularity, which can also be seen in the meson masses. For the η and σ coupling constants there is a second drop toward zero when the mass of these mesons approach $\omega_s = 2M_s$. In other terms, these two zeros signal the entrance into the continuum for u , d quarks and s quarks,

	T_{Mott}^π/T_c^χ	T_{Mott}^σ/T_c^χ	T_{Mott}^η/T_c^χ	T_{Mott}^K/T_c^χ
PNJL	1.07	0.95	0.98	1.06
NJL	1.08	0.82	0.92	1.07

TABLE III: Reduced Mott temperatures in the NJL and PNJL models at zero chemical potential.

respectively.

As already stated, the most striking difference between the NJL and PNJL models lies in the faster variation with the temperature of the PNJL results around any characteristic temperature. In particular, close to the phase transition, the NJL and PNJL calculations for the meson-quark coupling constants show a remarkable difference. We observe that, in both models, the mesons without flavor mixing (π and K) have a higher $T_{Mott}^{Meson}/T_c^\chi$ ratio than those with flavor mixing (η and σ) as it can be seen in Table III. It is interesting to note that, while $T_{Mott}^{Meson}/T_c^\chi$ for π and K does not change appreciably from one model to the other, for η and σ this ratio is higher in the PNJL model, where a faster decrease of the mixing effects is observed. This effect, which indicates a slightly longer survival of these mesons as bound states, is probably driven by the faster decrease of the strange quark mass, observed in the PNJL model.

The PNJL model is a quantitative step toward confinement with respect to the NJL quark model because the Φ factor suppresses the 1- and 2- quarks Boltzmann factor at low temperature. The fast restoration of the \mathbb{Z}_3 symmetry (Φ goes to one when temperature increases) producing, in a short range of temperatures, a quark thermal bath with all (1-, 2- and 3-) quark contributions might explain the fastening of the transition.

E. Topological susceptibility

We found it interesting to derive the topological susceptibility χ , which, in pure color SU(3) theory, is related to the η' mass through the Witten-Veneziano formula [36]

$$\frac{2N_f}{f_\pi^2}\chi = M_\eta^2 + M_{\eta'}^2 - 2M_K^2. \quad (22)$$

This observable, together with the mesonic masses and mixing angles, is strongly influenced by the anomaly: besides the degeneracy of the axial chiral partners and the recovery

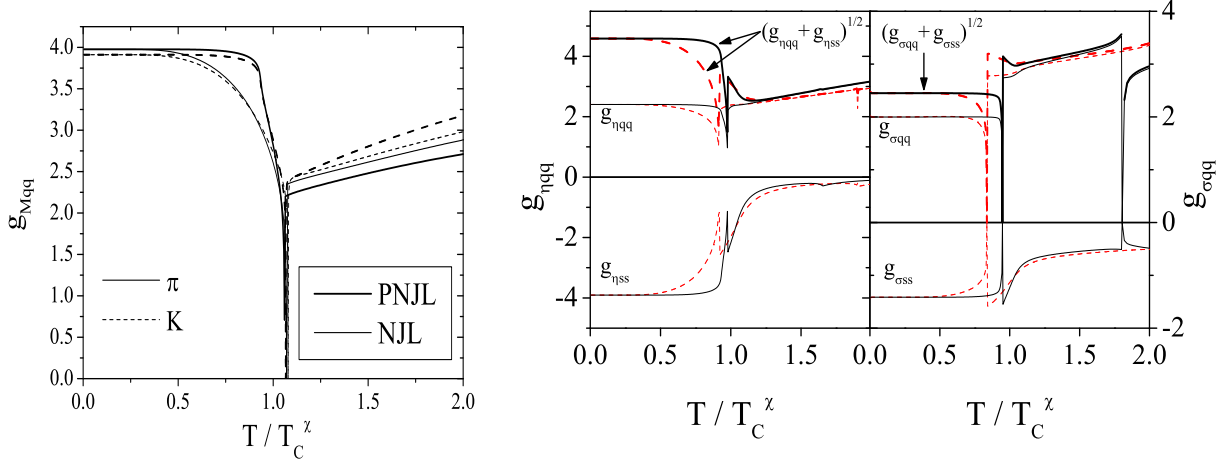


FIG. 4: The π , K (left panel) and η , σ (right panel) coupling constants as functions of the reduced temperature T/T_c^χ for the PNJL (solid lines) and NJL (dashed lines) models.

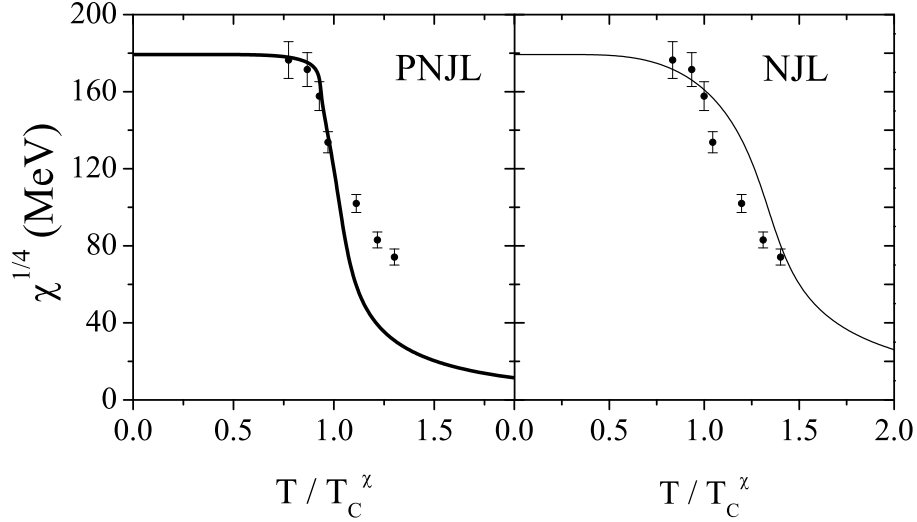


FIG. 5: Topological susceptibility as a function of the reduced temperature T/T_c^χ for the PNJL (left panel) and NJL (right panel) models.

of the OZI rule (mixing angles \rightarrow ideal values), the vanishing of χ is an indication of the absence of the anomaly and, consequently, of the effective restoration of the $U_A(1)$ symmetry. Lattice calculations indicate a strong decrease of the topological susceptibility with increasing temperature [37, 38, 39].

In Fig. 5 we show that, as expected from the previous analysis of the masses of the chiral partners and mixing angles, the axial symmetry is not fully restored at high temperatures, and the topological susceptibility is far away from being zero in both models (see Fig. 5). However, at $T = 2T_c^\chi$ the PNJL topological susceptibility is reduced to about 5% of its value at zero temperature, while the NJL one has a slower decrease. Moreover, it is interesting to notice that the PNJL calculation (without any change of the parameters previously fitted, or extra Ansatz, like the temperature dependence of the anomaly coefficient) nicely reproduces the first lattice points, namely, the rather steep drop around T_c^χ , while the NJL model fails to do so. The faster decrease of the topological susceptibility, the tendency of the mixing angles to approach earlier the ideal values and the reduction of the mass gap of the axial chiral partners, discussed in Sec. III C, are consistent indications that the Polyakov loop leads to a faster tendency to the restoration of the axial symmetry.

IV. SUMMARY AND CONCLUSIONS

In this work we have explored the thermodynamical properties of the vacuum state and the dynamics of the scalar-pseudoscalar meson spectrum propagating in a hot medium in the context of a $SU_f(3)$ PNJL model. Within the framework of such a model, we have included the flavor mixing and the coupling of quarks to the Polyakov loop, which in turn is governed by an effective potential.

Our results indicate that the main feature of the quark masses is a faster drop around T_c^χ in the PNJL model than in the NJL one. This indicates that the partial restoration of the chiral symmetry is more efficient and fast in the PNJL model. The mass of the strange quark in the PNJL model is still far from reaching the strange current quark mass even for high temperatures, although it exhibits a faster decrease than in the NJL model. This fact contributes to a faster decrease of the anomaly effects, with implications in the behavior of several observables.

We have observed that, qualitatively, the behavior of mesonic masses in the PNJL model is similar to the corresponding one in the NJL model. However, we notice that the mixing angle approaches the ideal angle faster in the PNJL model. In addition, the Mott temperatures are different in both models, showing that the domain where mesons with flavor mixing are bound states is extended in the PNJL model. These results show the relevance of the

effects of the interplay among $U_A(1)$ anomaly, the Polyakov loop dynamics, and the partial restoration of the chiral symmetry at finite temperature.

As a signal of the effective restoration of chiral symmetry in the nonstrange sector, the partners (π, σ) and (η, a_0) become degenerate, but this occurs at a lower reduced temperature in the PNJL model. On the contrary, in both models the η' and f_0 masses do not show a tendency to converge in the region of temperatures studied, an indication that chiral symmetry is not likely to be restored in the strange sector.

The comparative results of the meson-quark coupling constants are also interesting. In particular, close to the phase transition, the NJL and PNJL calculations for the meson-quark coupling constants show meaningful differences. In particular the σ and η mesons exhibit a tendency to a slightly longer survival as bound states.

Finally, there is a significative improvement in the PNJL model in the results concerning the topological susceptibility. At $T = 2T_c^x$ the latter is reduced to about 5% of its value at zero temperature, while in the NJL model it exhibits a slower decrease. Moreover, it is interesting to notice that the PNJL calculation nicely reproduces the first lattice points, with a rather steep drop around T_c^x , while this feature is not found in the NJL model. Although restoration of axial symmetry is not achieved, this behavior of the topological susceptibility (and of other relevant observables), indicates that the PNJL model shows a more efficient mechanism for the restoration of this symmetry.

Acknowledgments

Work supported by Grant No. SFRH/BPD/23252/2005 (P. Costa) and by F.C.T. under Project Nos. POCI/FP/63945/2005 and POCI/FP/81936/2007 (H. Hansen). This work was done in spite of the lack of support from Ministry of University and Research of Italy and France.

-
- [1] S. Datta, F. Karsch, P. Petreczky and I. Wetzorke, Phys. Rev. D **69**, 094507 (2004).
 - [2] E. Shuryak, Nucl. Phys. **A750**, 64 (2005).
 - [3] C.-Y. Wong, Phys. Rev. C **72**, 034906 (2005).
 - [4] W.M. Alberico, A. Beraudo, A. De Pace and A. Molinari, Phys. Rev. D **72**, 114011 (2005).

- [5] Á. Mócsy and P. Petreczky, Phys. Rev. D **73**, 074007 (2006).
- [6] P. Costa, M. C. Ruivo, C. A. de Sousa, and Yu. L. Kalinovsky, Phys. Rev. D **70**, 116013 (2004); Phys. Rev. D **71**, 116002 (2005).
- [7] H. Hansen, W. M. Alberico, A. Beraudo, A. Molinari, M. Nardi, and C. Ratti, Phys. Rev. D **75**, 065004 (2007).
- [8] P. N. Meisinger and M. C. Ogilvie, Phys. Lett. B **379**, 163 (1996).
- [9] P. N. Meisinger, T. R. Miller, and M. C. Ogilvie, Phys. Rev. D **65**, 034009 (2002).
- [10] R. D. Pisarski, Phys. Rev. D **62**, 111501(R) (2000); R. D. Pisarski, hep-ph/0203271.
- [11] Kenji Fukushima, Phys. Lett. B **591**, 277 (2004).
- [12] Á. Mócsy, F. Sannino and K. Tuominen, Phys. Rev. Lett. **92**, 182302 (2004).
- [13] C. Ratti, M. A. Thaler, and W. Weise, Phys. Rev. D **73**, 014019 (2006); C. Ratti, M. A. Thaler and W. Weise, nucl-th/0604025.
- [14] E. Megías, E. R. Arriola, and L.L. Salcedo, Phys. Rev. D **74**, 065005 (2006); Phys. Rev. D **74**, 114014 (2006).
- [15] S. Rößner, C. Ratti, and W. Weise, Phys. Rev. D **75**, 034007 (2007).
- [16] C. Sasaki, B. Friman, and K. Redlich Phys. Rev. D **75**, 074013 (2007).
- [17] S. K. Ghosh, T.K. Mukherjee, M. G. Mustafa, and R. Ray, Phys. Rev. D **73**, 114007 (2006).
- [18] B.-J. Schaefer, J. M. Pawłowski, and J. Wambach, Phys. Rev. D **76**, 074023 (2007).
- [19] S. Weinberg, Phys. Rev. D **11**, 3583 (1975).
- [20] G. 't Hooft, Phys. Rev. Lett. **37**, 8 (1976); Phys. Rev. D **14**, 3432 (1976).
- [21] Wei-jie Fu, Z. Zhang, and Yu-xin Liu, Phys. Rev. D **77**, 014006 (2008).
- [22] M. Ciminale, R. Gatto, N.D. Ippolito, G. Nardulli, and M. Ruggieri; Phys. Rev. D **77**, 054023 (2008).
- [23] Kenji Fukushima, Phys. Rev. D **77**, 114028 (2008).
- [24] A. M. Polyakov, Phys. Lett. B **72**, 477 (1978).
- [25] G. 't Hooft, Nucl. Phys. **B138**, 1 (1978).
- [26] B. Svetitsky and L. G. Yaffe, Nucl. Phys. **B210**, 423 (1982).
- [27] P. N. Meisinger, M. C. Ogilvie and T. R. Miller, Phys. Lett. B **585**, 149 (2004).
- [28] O. Kaczmarek, F. Karsch, P. Petreczky, and F. Zantow, Phys. Lett. B **543**, 41 (2002).
- [29] O. Kaczmarek, PoS **CPOD07**, 043 (2007).
- [30] P. Costa, M. C. Ruivo, C. A de Sousa and Yu. L. Kalinovsky, Phys. Rev. C **70**, 025204 (2004).

- [31] S. P. Klevansky, *Rev. Mod. Phys.* **64**, 649 (1992).
- [32] P. Rehberg, S. P. Klevansky and J. Hüfner, *Phys. Rev. C* **53**, 410 (1996).
- [33] P. Zhuang, J. Hüfner and S. P. Klevansky, *Nucl. Phys.* **A576**, 525 (1994).
- [34] P. Costa, M. C. Ruivo, and C. A de Sousa, *Phys. Rev. D* **77**, 096009 (2008).
- [35] P. Costa, M. C. Ruivo and Yu. L. Kalinovsky, *Phys. Lett. B* **560**, 171 (2003).
- [36] E. Witten, *Nucl. Phys.* **B156**, 269 (1979); G. Veneziano, *Nucl. Phys.* **B159**, 213 (1979).
- [37] B. Allés, M. D’Elia, and A. Di Giacomo, *Nucl. Phys.* **B494**, 281 (1997).
- [38] M.-C. Chu, S. M. Ouellette, S. Schramm, R. Seki, hep-lat/9712023; B. Allés, M. D’Elia, A. Di Giacomo, P.W. Stephenson, *Nucl. Phys. (Proc. Suppl.)* **73**, 518 (1999).
- [39] B. Allés, M. D’Elia, M. P. Lombardo and M. Pepe, *Nucl. Phys. (Proc. Suppl.)* **94**, 441 (2001).
- [40] J. Schaffner-Bielich and J. Randrup, *Phys. Rev. C* **59**, 3329 (1999).
- [41] J. Schaffner-Bielich, *Phys. Rev. Lett.* **84**, 3261 (2000).
- [42] J. T. Lenaghan, D. H. Rischke and J. Schaffner-Bielich, *Phys. Rev. D* **62**, 085008 (2000).
- [43] B.-J. Schaefer and M. Wagner *Phys. Rev. D* **79**, 014018 (2009).
- [44] D. Horvatić, D. Klabucar and A. E. Radzhabov *Phys. Rev. D* **76**, 096009 (2007).